DOI:10. 12119 / j. yhyj. 202002010

Study on the Separation Process of Aluminum and Lithium by Nanofiltration

GAO Lin[1,2,3], WANG Huai - you[1,2], ZHAO You - jing[1,2], WANG Min[1,2]

(1. *Key Laboratory of Comprehensive and Highly Efficient Utilization of Salt Lake Resources, Qinghai Institute of Salt Lakes, Chinese Academy of Sciences, Xining*, 810008, *China*; 2. *Key Laboratory of Salt Lake Resources Chemistry of Qinghai Province, Xining*, 810008, *China*; 3. *University of Chinese Academy of Sciences, Beijing*, 100049, *China*)

Abstract: This paper concerns the feasibility of nanofiltration separation of Al^{3+} and Li^{+}, and a new method for separating and recovering lithium from lepidolite leaching solution was proposed. Factors like salinity and mass ratio of Al^{3+}/Li^{+} were developed during the separation. The investigation on salinity indicated that the retention rate of Al^{3+} and Li^{+} decreases with incremental salinity. Li^{+} invariably exhibits a negative concentration gradient diffusion and the retention rate of Al^{3+} can be stabilized above 99%. Separation factor of Al^{3+}/Li^{+} has arrived 248. 333 at the salinity is 45 g/L, and the corresponding zeta potential on the membrane also reaches a maximum value. In the experiments with different Al^{3+}/Li^{+} mass ratios, inflection points has appeared in the retention rate of Al^{3+} and Li^{+} at different ratios. The pH of solution appeared to decrease first, then increase and finally decrease. Overall, this paper has found that DK membrane has a high rejection rate of aluminum and a relatively good separation efficiency and provided a novel vision for future separation of lithium and aluminum from lepidolite leaching solution.

Key words: Nanofiltration; Aluminium separation; Lithium recovery; Zeta potential; Lepidolite leaching solution

CLC number: TS353 **Document code**: A **Article ID**: 1008 - 858X(2020)02 - 0079 - 12

1 Introduction

Lithium, as a paramount energy element of the 21st century, is widely used in lithium batteries, nuclear power, aerospace and space applications, medical and so on[1-6]. It is mainly stored in brines and lithium-containing ores [7,8]. Most of lithuim is currently derived from spodumene and brines, however, as the tremendous demand in lithium batteries and other products, lepidolite could be considered as a promising resources to extract lithium.

At present, there are two main methods for extracting lithium froml epidolite and the principle of both methods is that the displacement reaction occurs under different conditions to transfer lithium out of the insoluble aluminosilicate phase. One method is that the ore first undergoes a crystal phase transformation at high temperature, and then the solid phase is successfully subjected to a leaching process to obtain a lithium-containing solution, such as chlorination roasting method [9-11] and sulfate method [12-15]. Another is the ore reacts directly with solution, and lithium in the solid phase is displaced into the solution,

Received date: 2019 - 12 - 12

such as hydrofluoric acid method and sulfuric acid method [16]. The sulfuric acid method is exceedingly cumbersome to remove aluminum from the leachate, so many researchers have made a lot of attempts on the removal of aluminum ions, including the addition of acids, alkali and extractant to liquids [17-19]. The process tend to be more complicated and the extraction efficiency of Li also decreased due to the addition of chemicals. Another inherent disadvantage is the generation of large amounts of waste. Since nanofiltration is relatively mature in the separation of lithium from brine, we attempts to remove Al^{3+} from lepidolite leaching solution by nanofiltration.

Nanofiltration was first proposed by J. E. Cadotte in the field of seawater treatment under the help of FilmTec Corporation [20]. It is a separation by which molecules are sieved and diffused through a selective layer of the nanofiltration membrane. Compared to other pressure driven membrane separation processes, such as ultrafiltration, microfiltration, reverse osmosis, the role of surface charge is more important in nanofiltration[21]. As a powerful tool for separating small molecules and salts, nanofilration has attracted increasingly attention in many applications like wastewater treatment[22-24] and water purification[25] Additionally, it has been widely used in the extraction of lithium from salt lakes with high magnesium to lithium ratio [26-29].

Nanofiltration is also commonly used for the removal of heavy metal ions in industrial wastewater. Lou et al. [30] used membrane separation technology to recover the electroplated nickel rinsing water and showed that the retention rate of Ni^{2+} by first-class nanofiltration can reach more than 97%. Wang et al. [31] investigated the removal of Cr and Cu by using NTR-7450, DL and DK nanofiltration membrane, the experiment found that the DK film has the best resistance to acidic electroplating wastewater, with a rejection rate of 96.6% for Cr and a rejection rate of 90% for Cu. Huang et al. [32] found that the separation of Cr by the nanofiltration membrane was affected by the morphology of Cr ions, the operating pressure, and the mass concentration of the feed liquid. Zhong et al. [33] found that the retention rate of heavy metal ions by nanofiltration membranes was higher than 97% whenused DK nanofiltration membrane to separate sulfuric acid waste liquid containing Fe^{3+}, Mn^{2+}, Zn^{2+} and Al^{3+}, and found that the interception rate of the four metal ions could reach above 96%.

To save operating cost and enhance lithium recovery from the ores, a novel process was introduced in this paper to separate aluminium and lithium of lepidolite leaching solution by nanofiltration. Consequently, the possibility of separating Al^{3+}/Li^{+} by nanofiltration was preliminarily explored under different operating conditions in Al^{3+}, $Li^{+}/Cl^{-}/H_2O$ system in this study. Based on our previous research and other researchers's literatures on the retention of ions by several nanofiltration membranes, this experiment chose DK nanofiltration membrane with better separation efficiency.

Table 1 Ions retention of several membranes in the literatures

Membrane	Retention rate		Literature
	Li	Others	
DL	-85%	Mg: 61% ~67%	Wen et al. [28]
DK	-75%	Mg: 90%	Li et al. [26]
NF	-	Al: >78%	Kettunen et al. [35]
	15%	95%	Somrani et al. [36]
	-	Cr(III): 35%	Huang et al. [37]

2 Materials and Methods

2.1 Preparation of feed

It was well-known that theanion of lepidolite leaching solution based the sulfuric acid method was SO_4^{2-}. Due to SO_4^{2-} cannot pass through nanofiltration membrane, so Ba^{2+} or Ca^{2+} can be added to remove or partially remove SO_4^{2-} from the solution in the actual production. In this paper, SO_4^{2-} was removed completely in order to study the separation effect and separation mechanism of Al^{3+}/Li^{+}. Synthetic lepidolite leaching solution without SO_4^{2-} was prepared by dissolving aluminum chloride hexahydrate and lithium chloride monohydrate.

All the reagents were supplied by Sinopharm Chemical Reagent Co., Ltd, China. Aluminum chloride hexahydrate ($AlCl_3 \cdot 6H_2O$, AR, 97%) and lithium chloride monohydrate ($LiCl \cdot H_2O$, AR, 97%) were used as received. Deionized water (resistivity, 18.25 MΩ · cm) was obtained by an ultrapure water machine (UPT – II – 20T, Chengdu Ultrapure Technology Co., Ltd, China).

Separation experiments were performed under different salinity (15, 25, 35, 45, 55 g/L) and $r_{Al/Li}$ (mass ratio of Al^{3+}/Li^{+}: 3, 6, 15, 25, 35). Table 2 shows the operating conditions of separation experiments. Concentrate and permeate solution were obtained after equilibration of the membrane system for 10 minutes. The device was thoroughly rinsed with salt solution before each experiment run 3 times to ensure that there is no residual water in the instrument. Also be rinsed the membrane unit 3 times with deionized water at the end of each experiment. No concentrate and permeate was circulated in the experiment. Each experiment was repeated for three times to improve the accuracy and error bars were added to the graphs.

Table 2 Experimental operating conditions

	P /MPa	*L* /LPM	*T* /K	Salinity /(g/L)	$r_{Al/Li}$
Salinity	3.4	3.5	293.15	15 25 35 45 55	6
$r_{Al/Li}$	3.4	3.5	293.15	45	3 6 15 25 35

2.2 Seperation set-up

A lab-scalenanofiltration unit device (DSP – 1812W – S, Hangzhou Donan Memtec Co., Ltd. China) was used for the nanofiltration experiments. The membrane was located in a radial flow circular unit with the feed entering the center of the membrane and flowing radially outward (Fig. 1). Pressures and flows were interrelated, which were set by manual valves. If the temperature of the circulating liquid exceeded a set value, the heat exchanger starts to work and the temperature decreased. The

concentrate stream J_c that had not passed through the membrane can be recycled to the feed. The permeate stream J_p can be removed or recycled to the feed tank. Sampling can be done in the feed tank and from permeation flow.

2.3 Membrane

The spiral-wound nanofiltration membrane (DK-1812, General Electric Company, USA) used in this experiment has the characteristic of retaining multivalent ions while penetrating monovalent ions, in which a polyamide selective layer is supported on a polysulfone layer. The following process parameters are recommended by the manufacturer: operational temperature range 283 ~ 323 K; pH 2 ~ 11 during processing and pH 2.5 ~ 10.5 during cleaning; maximum pressure of 3.5 MPa during processing; effective membrane area 0.38 m^2. In addition, in order to further study the separation mechanism of ions, a series of essential tests about surface hydrophilicity and membrane charge have been carried out on the surface properties of the membrane, just as Table 3 shows[38]

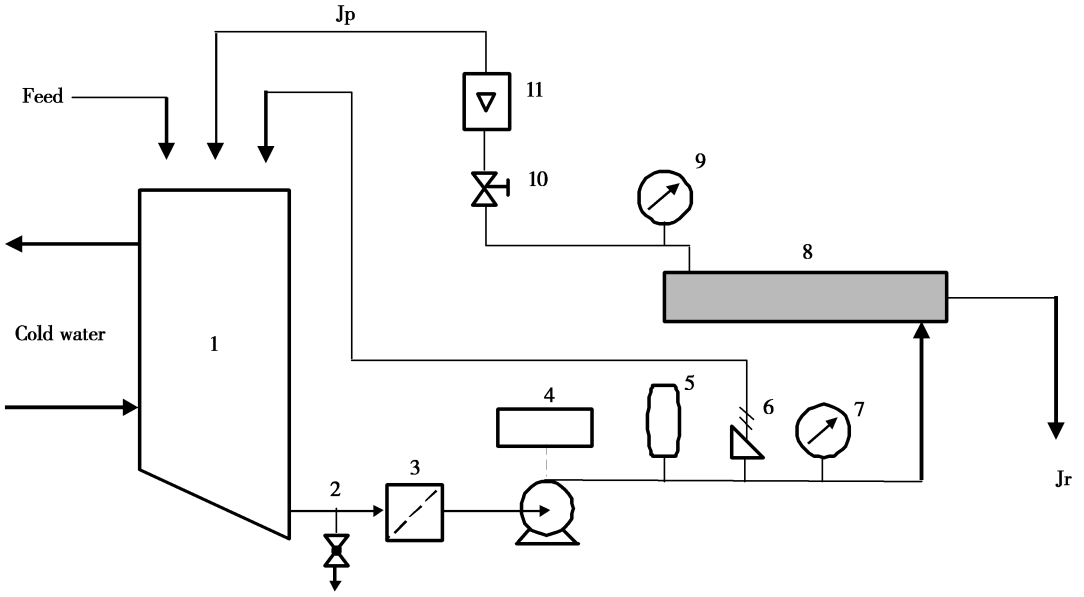

1 Circulating tank; 2 Drain valve; 3 Pipeline filter; 4 Pump; 5 Frequency converter; 6 Safety relief valve; 7 Pressure gauge; 8 membrane; 9 Pressure gauge; 10 Pressure regulating valve

Fig. 1 Experimental set-up of the nanofiltration separation

Table 3 Characterization methods for membrane

Characterization methods	Membrane characteristics	Instrument
Contact angle measurements	Surface hydrophilicity	DSA30, Kruss
Zetapotential measurements	Membrane charge	Supass, Anton Paar
Mathematical modeling based on solute retention data	Pore size; membrane thickness	–

2.4 Analysis and measurement

Concentration of cations in the solution was measured by inductively coupled plasma-optical emission spectrometry (ICP-OES). Other measurements for the required data are shown in Table 4.

Table 4　Instruments required

Parameter	Model	Instrument
Li^+	ICAP6500 spectrometer	Thermo Scientific
Al^{3+}	ICAP6500 spectrometer	Thermo Scientific
Organic molecules content	TOC – L	Shimadzu
T	Infrared thermometer GM320	Benetech
pH	pH meter S210	Mettler Toledo
Viscosity	Digital rotary viscometer NDJ – 8S	Shanghai Jingke

2.5 Calculation

Retention rate, R, refers to the permeability of ions, which is the main indicator for evaluating its separation ability.

$$R = \left(1 - \frac{C_P}{C_F}\right) \times 100\% \quad (1)$$

Where C_p and C_f are, respectively, the concentration of ions of the permeate and feed solution, (g/L).

Separation factor, SF, means the ratio of the mass ratio of Li^+ and Al^{3+} in the permeate and the feed solution.

$$SF = \frac{(C_{Li^+}/C_{Al^{3+}})_P}{(C_{Li^+}/C_{Al^{3+}})_F} \quad (2)$$

When $SF > 1$, lithium ions preferentially pass through the membrane to be enriched. The larger the value is, the better the separation effect.

Permeate flux, J, refers to the volume of permeate permeated through the effective membrane area per unit time, reflecting the ability of the composite membrane to handle a certain concentration of solution.

$$J = \frac{V}{t \cdot S \cdot 3600} \quad (3)$$

Where V is the volume ofthe permeate, L; S is the effective area of the diaphragm, m^2; and t is the time taken for sampling, h.

3 Result and discussions

3.1 Characterization of membranes

3.1.1 Zeta potential of the membrane

When the membrane is in contact with the electrolyte solution, an electric double layer of the diffusion layer and the dense layer may be formed at the membrane-liquid interface. The boundary between the two layers is a sliding surface, and the potential on the sliding surface is named as zeta potential. The charge performance of the surface can be characterized by measuring the zeta potential[39]

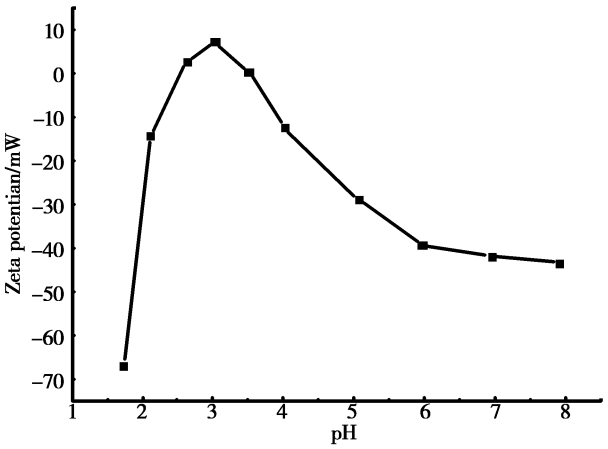

Fig. 2　Isopotential point curve of DK membrane

The zeta potentialwas displayed as a pH – ζ curve at a pH between 3 to 10. When ζ = 0, the charging effect disappears, and the corresponding

pH is 3.52. ζ increases first and then decreases with increasing pH, and it is positive near the isopotential point (IEP).

3.1.2 The pure water permeability of the membrane

L_p as an important membrane structure parameters, is only related to the temperature. Standard procedures were followed for membrane charaterization with pure water: the transmembrane flux was measured at an applied pressure range of 2.1 ~ 3.4 MPa at 293.15 K. The average water permeability was calculated as 1.192×10^{-11} m · s^{-1} Pa^{-1} by (3 – 1)[40], which is consistent with previous literature [41].

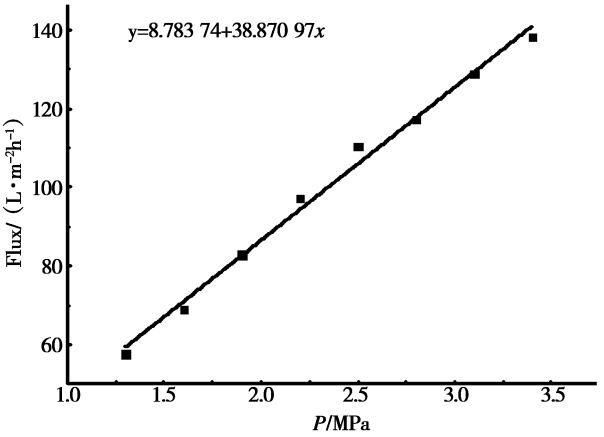

Fig. 3 The pure water permeability of the membrane

$$J_W = L_P(\triangle P - \sigma\triangle\pi) \quad (4)$$

Where J_V is the water flux; ΔP is the applied pressure; L_p is the pure water permeability; σ is the reflection coefficient; and $\Delta\pi$ is the osmotic pressure, however, when we are talking about pure water, $\Delta\pi = 0$.

3.1.3 Pore radius

Organic molecules are removed by a sieving mechanism, based on the small pore size of the membrane. The membranes pore size are often characterized by the molecular weight cut-off: the molecular weight of a molecule which is retained for 90% [42]. The effective pore radius r_p (nm) of composite membrane was evaluated by the Steric-hindrance pore model that reported in previous study. Using the data in the Table 5, the regression curve of the organic molecular Stokes radius and molecular weight is established as shown in Fig. 5, an equation is obtained as (5) [43]. Based on Steric – hindrance pore model, r_p can be estimated as 0.446 nm.

$$r_s = 0.04673\ MW^{0.3971} \quad (5)$$

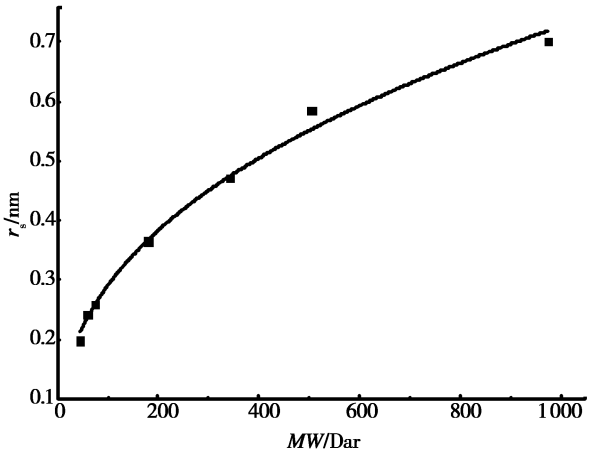

Fig. 4 Correlation between Stokes radius and molecular weight of neutral molecules

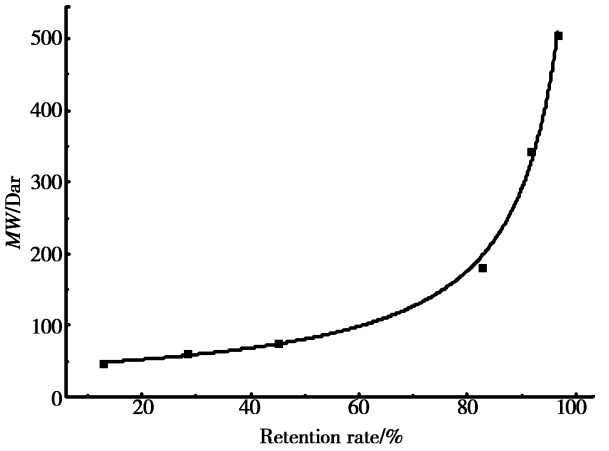

Fig. 5 The retention of different neutral molecules with different molecular weight

3.2 Separation of Al^{3+}/Li^{+} at different salinity

When the operating temperature and operating pressure were kept at 293 K and 3.4 MPa, respectively, and the initial mass ratio of aluminum to lithium was maintained at 6, the observation that the salinity of the solution changes between 15 ~ 55 g/L was shown in Fig. 6. The retentions of ions depend on the valence, concentration, and chemical nature of the compounds in solution, as well as the surface

charge, charge density, and chemical nature of the group on the membrane surface[21]. At the micro level, the separation mechanism is the combination of steric hindrance, Donnan exclusion and dielectric exclusion (DE) between ions and the fixed groups of the membrane [44,45]. As the feed concentration increases, the cations on the surface of the membrane will enhance the DE exclusion, and the shielding effect of the adsorbed counter ions on the fixed charge weakens the Donnan exclusion [28].

Fig. 5　Molecular weight of neutral molecules and their Stokes radius

Solute	Ethanol	Isopropanol	n-Butanol	Glucose	Sucrose	Raffinose	α – Cyclodextrin
MW	46.07	60.06	74	180.16	342.30	504.42	972.84
r_s	0.198	0.241	0.258	0.365	0.471	0.584	0.701

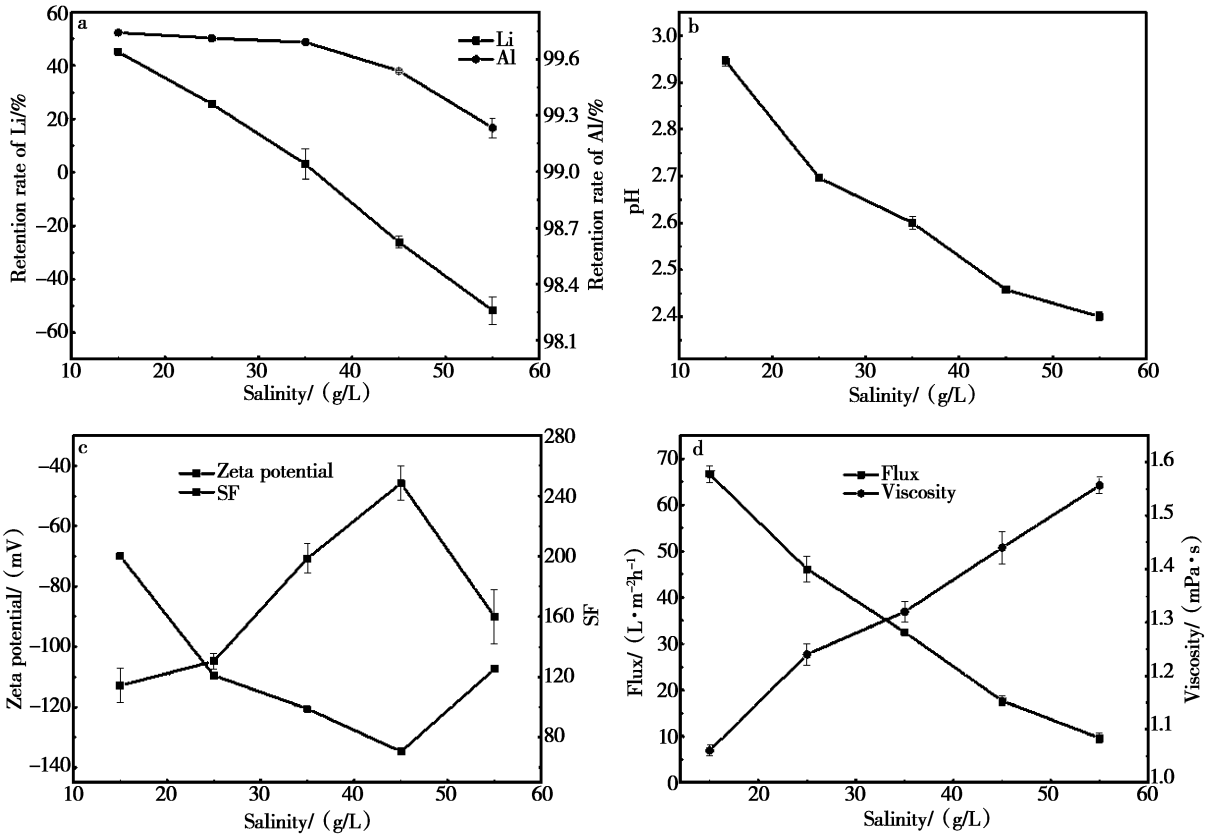

Fig. 6　Effect of salinity on the separation

It can be seen from the Fig. 6a the retention rate of Al^{3+} by the DK membrane is above 99% whatever the salinity is, and steric hindrance plays a leading role in the retention of Al^{3+}. This is not only due to the large hydration radius of aluminum ions, but also the complicated complex formed by Al^{3+} and water, resulting in the polymerization of polynuclear aluminum in solution.

The radius of Al^{3+} is 0.439 nm, which is close to the pore size of the membrane, 0.446 nm, and the radius will be larger than the pore size of the membrane after hydration. As salinity increase, the

retention of Al^{3+} shows a slight downward trend and more Al^{3+} will be 'pushed' through the membrane because of concentration polarization. Besides, Li^+ has passed through the membrane under negative concentration gradient as Fig. 6a signified. And the negative retention rate of Li^+ basically shows a almost linear decrease trend with the increase of salinity, it can finally reach to -51.7% when the salinity is 55 g/L. It is the same as the retention tendency of the monovalent ions described in the prior literature [46,47]. Since Li^+ has a smaller hydration radius and a larger diffusion coefficient, it is easy that Li^+ diffuses toward the other side of the membrane. It is firstly carried by a large amount of Cl^- and by driving force of potential difference to maintain electrical neutrality.

Table 6 Ionic radius and diffusion coefficient of various ions [48,49]

Ion	*AW* /g mol^{-1}	r_s /nm	D_∞ /(m^2 s^{-1}) × 10^{-9}
Li^+	6.941	0.238	1.03
Al^{3+}	26.982	0.439	–
Cl^-	35.45	0.121	2.03

As shown in Fig. 6b, the decrease in pH of the solution is due to the fact that more OH^- are combined with increased aluminum ions, resulting in the increase of free H^+ in the solution. Influence of zeta potential on the surface charge distribution is a key factor affecting the ion transport process. The chargeability of membrane surface is depends on the feed pH, as well as the type and concentration of electrolyte [50], therefore, this experiment has measured the zeta potential in different solutions. And it was found to be less stable during the measurement because of the longer time required for the formation of the electric double layer in the high concentration solution [51]. Therefore, in order to obtain a more accurate potential value, potential of the membrane surface is measured multiple times. The test results indicate the membrane surface is negatively charged at different salinity at a pH between 2.5 and 3.2, which is totally opposite of the IEP diagram (Fig. 3). There are two causes contributing to the change in charging performance, one of which is that the cation is more hydrated than the anion[39], and the larger diffusion coefficient of Cl^- is another reason. Therefore, a large amount of Cl^- is adsorbed on the surface of the membrane in the solution.

The Zeta potential increases first and then decreases as Fig. 6c shows. Higher salinity makes more Cl^- to be adsorbed on the surface of the membrane, so that the value of zeta potential has increased to 134.7 mV. Nevertheless, more Al^{3+} has been accumulated on the surface of the membrane on account of concentration polarization, which decreases the zeta potential then. Charge effect between cations and Cl^- on the surface will be weakened correspondingly. The trend of SF and zeta potential are exactly the same (Fig. 6c), because the larger the negative electromotive force on the surface, the easier the transmission of Li^+, so the SF reaches the maximum 248.333 when the electromotive force is the largest at 45 g/L. The decrease in the zeta potential causes the driving force of the counter ion adsorbed on the membrane to pass through the membrane to reduce, so the SF tends to decrease. This also indicates that the charge performance of the film surface plays a decisive role in the separation of Al^{3+}/Li^+.

Fig. 6d has shown the viscosity of the solution increases slightly and the corresponding flux renders an opposite decrease from 67 to 10 L · $m^{-2}h^{-1}$ with incremental salinity. The more Al^{3+} accumulated on the surface of the membrane, the stronger the polarization of Al^{3+} concentration, which increases the resistance of Li^{+} permeation.

3.3 Separation of Al^{3+}/Li^{+} at different $r_{Al/Li}$

When the working temperature and working pressure are maintained at 296.15 K and 3.4 MPa, respectively, the fixed salinity is optimal 45 g/L and the mass ratio of aluminum to lithium in the feed solution is changed. The observation of the experiment in which the mass ratio of aluminum to lithium varies between 3 ~ 35 is shown in Fig. 7. It can be seen from Fig. 7a that the retention of Al^{3+} first increases and then decreases, but remains stable at more than 99%. Because sieving mechanism plays a leading role in the separation of aluminium and lithium. Therefore, this work does not take into account the effect of complex morphological distribution of aluminum ions in high salinity solutions on separation.

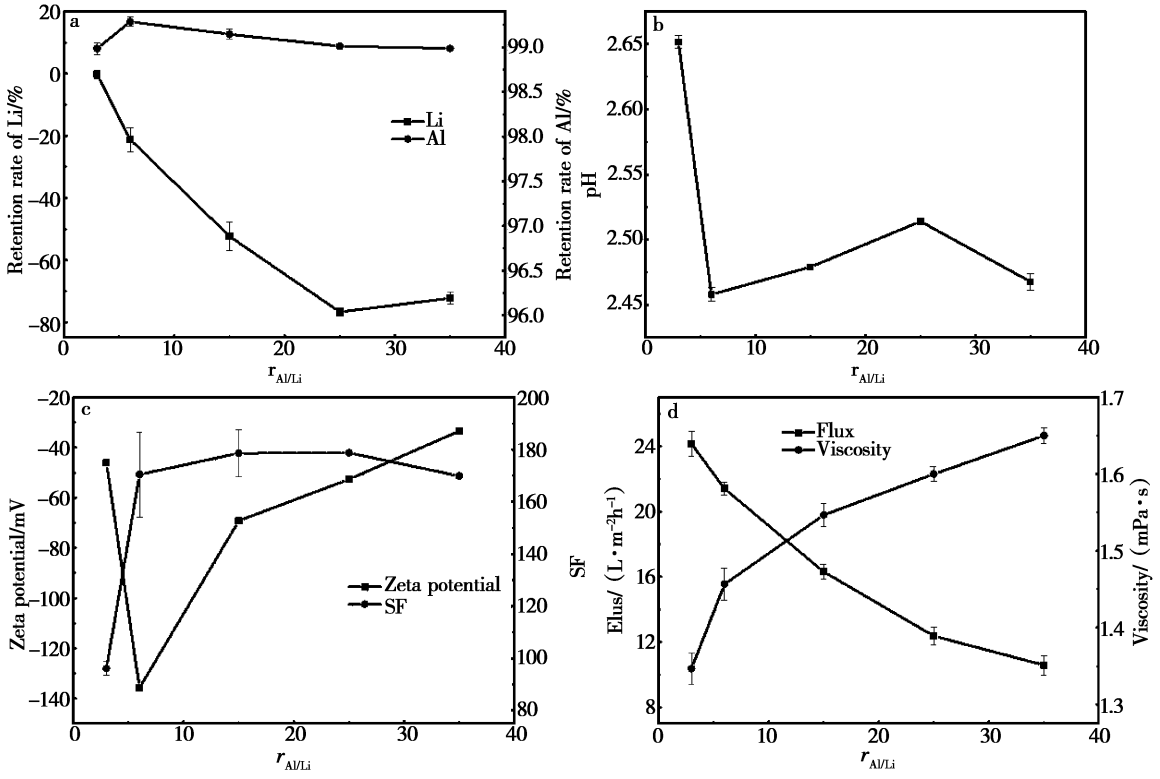

Fig. 7　Effect of $r_{Al/Li}$ on the separation

When the $r_{Al/Li}$ is 6, the retention of Al^{3+} decreases after reaching a maximum of 99.28%, and Fig. 7c shows that the corresponding zeta potential reaches a maximum of −134.835 mV. This is because when the surface charge of the membrane is large, DE affects the transmission of Al^{3+} in addition to the sieve effect. At the interface between the extra-membrane solution and the membrane pore solution, DE is produced due to the difference in ion dielectric constant. Repulsive energy is proportional to the square of the ionic charge including cations and anions [52]. Therefore, the zeta potential has an opposite tendency to the retention of Al^{3+}.

The retention of Li^{+} reaches a minimum to −76.7% when $r_{Al/Li}$ is 25, and then rises slightly while the transmission of Li^{+} depends only on the

charge effect and the concentration polarization (Fig. 7a). The resistance of Li^+ through the membrane increases when $r_{Al/Li}$ is 35 because more aluminum is retained and accumulates on the membrane surface as the aluminum content in the solution increases.

As $r_{Al/Li}$ increases, pH decreases first, then increases and then decreases (Fig. 7b). This complex variation is due to the presence of zwitterionic Al^{3+}. Since more OH^- in the solution is bonded by Al^{3+}, the pH is lowered. However, the increase of pH is owing to the amount of Al^{3+} present in the solution with the increase of $r_{Al/Li}$, and Al^{3+} forms its own polynuclear aluminum polymer.

Zeta potential is considerably affected by pH. When $r_{Al/Li}$ is 6, pH reaches a minimum of 2.458, and the zeta potential reaches maximum value. Since hydrated aluminum has a lower charge and a larger radius than Al^{3+}, the effect of aluminum on the surface charge of the membrane is further reduced, and zeta potential reaches a maximum due to the large amount of Cl^- on the surface of the membrane. After that, as rising of the ratio of aluminum to lithium, more aluminum accumulates on the surface of the membrane, which inevitably leads to a continued decrease of the surface charge of the membrane. SF first rises rapidly when the $r_{Al/Li}$ increase from 3 to 6, then the upward trend slows down, and decreases after reaching a maximum of 178.74 at a $r_{Al/Li}$ of 25 (Fig. 7c). As with the salinity experiment, the variational trend of SF is still consistent with zeta potential, which again proves that the surface charge plays a decisive role in the transmission of Li^+ and Al^{3+}.

The viscosity of the solution increases significantly with the increasing of $r_{Al/Li}$ when the salinity is 45 g/L because of the presence of aluminum polymer in the solution. And the flux of the permeate solution decreases slightly.

4 Conclusion

This study developed nanofiltration as a new method for extracting lithiumfrom lepidolite leaching solution. The effect of salinity and $r_{Al/Li}$ on the separation of $AlCl_3$/LiCl system was carried out. Moreover, the salinity and $r_{Al/Li}$ have been confirmed to have a considerable influence on the separation, mainly because the surface charge of the membrane is different in different solutions. And slight changes will affect the charge partitioning, Donnan exclusion and dielectric exclusion, on the membrane surface to change the Al^{3+}/Li^+ transmittance property. In this experiment, Al^{3+} in this artificial leaching solution was almost completely removed by nanofiltration separation, which provided a new way to seek a more environmentally friendly and effective method for extracting lithium from lepidolite leaching solution.

References:

[1] Tarascon J M, Armand M. Issues and challenges facing rechargeable lithium batteries[J]. Nature, 2001, 414(6861): 359 – 67.

[2] Batistoni P, Angelone M, Carconi P, *et al.* Neutronics experiments on HCPB and HCLL TBM mock-ups in preparation of nuclear measurements in ITER[J]. Fusion Engineering and Design, 2010, 85(7 – 9): 1675 – 1680.

[3] Xu W, Birbilis N, Sha G, *et al.* A high-specific-strength and corrosion-resistant magnesium alloy[J]. Nat Mater, 2015, 14(12): 1229 – 35.

[4] Rioja R J, Liu J. The Evolution of Al-Li Base Products for Aerospace and Space Applications[J]. Metallurgical and Materials Transactions a-Physical Metallurgy and Materials Science, 2012, 43a(9): 3325 – 3337.

[5] Daneshmand A, Mohammadi H, Rahimian R, *et al.* Chronic lithium administration ameliorates 2,4,6 – trinitrobenzene sulfonic acid-induced colitis in rats; potential role for adenosine triphosphate sensitive potassium channels[J]. J Gastroenterol Hepatol, 2011, 26(7): 1174 – 81.

[6] De Laurentis N, Cann P M, Lugt P M, *et al.* The Influence of Base Oil Properties on the Friction Behaviour of Lithium Greases in Rolling/Sliding Concentrated Contacts[J]. Tribology Letters, 2017, 65(4): 128.

[7] Shi Dong L L – J, Li Jin – Feng, Ji Lian – Min, Song Fu – Gen, Peng Xiao – Wu, Zhang Li – Cheng, Zhang Yu – Ze, Li Hui – Fang, Song Xue – Xue, Nie Feng, Zeng Zhong – Min, Liu Zhi – Qi, Guo Fan. Extraction of Lithium from Salt Lake Brine using N523 – TBP Mixture System[J]. 盐湖研究, 2019, 27(02): 95 – 110.

[8] Grosjean C, Miranda P H, Perrin M, *et al.* Assessment of world lithium resources and consequences of their geographic distribution on the expected development of the electric vehicle industry[J]. Renewable & Sustainable Energy Reviews, 2012, 16(3): 1735 – 1744.

[9] Yan Q – X, Li X – H, Wang Z – X, *et al.* Extraction of lithium from lepidolite using chlorination roasting-water leaching process[J]. Transactions of Nonferrous Metals Society of China, 2012, 22(7): 1753 – 1759.

[10] El – Obeid H A, Al – Badr A A. Mestranol[J]. 1982, 11: 375 – 406.

[11] Barbosa L I, Gonzalez J A, Ruiz M D. Extraction of lithium from beta-spodumene using chlorination roasting with calcium chloride[J]. Thermochimica Acta, 2015, 605: 63 – 67.

[12] Kuang G, Liu Y, Li H, *et al.* Extraction of lithium from β – spodumene using sodium sulfate solution[J]. Hydrometallurgy, 2018, 177: 49 – 56.

[13] Luong V T, Kang D J, An J W, *et al.* Iron sulphate roasting for extraction of lithium from lepidolite[J]. Hydrometallurgy, 2014, 141: 8 – 16.

[14] Luong V T, Kang D J, An J W, *et al.* Factors affecting the extraction of lithium from lepidolite[J]. Hydrometallurgy, 2013, 134: 54 – 61.

[15] Yan Q X, Li X H, Wang Z X, *et al.* Extraction of valuable metals from lepidolite[J]. Hydrometallurgy, 2012, 117: 116 – 118.

[16] Guo H, Kuang G, Wang H, *et al.* Investigation of Enhanced Leaching of Lithium from α – Spodumene Using Hydrofluoric and Sulfuric Acid[J]. Minerals, 2017, 7(11): 205.

[17] Xu M, Sun X, Zhao Q. Alum recovery fromwaterworks sludge by solvent extraction using Bi – (2 – eth – ylhexyl) phosphate Ⅱ Slurry extraction[J]. Journal of East China University of Science and Technology (Natural Science Edition), 2007, 33(3): 375 – 378.

[18] Jia J, Zhang Y, Sheng W U, *et al.* Distribution and Separation of Aluminum in the Rare Earth Solvent Extraction Separation Processes(I)[J]. Chinese Rare Earths, 2001.

[19] Ma Y, Zhu T. Aluminum extraction dynamic investiga-tion in HCl system by solvent extraction using Bi – (2 – eth – ylhexyl) phosphate [J]. Chinese Journal of Nonferrous Metals, 1992(4): 26 – 32.

[20] J. E. Cadotte C V K K E C, And L. T. Rozelle. In Situ-Formed Condensation Polymers for Reverse osmosis Membranes: Second Phase[R]. Springfield, VA: National Technical Information Service, 1974.

[21] Manttari M, Pihlajamaki A, Nystrom M. Effect of pH on hydrophilicity and charge and their effect on the filtration efficiency of NF membranes at different pH[J]. Journal of Membrane Science, 2006, 280(1 – 2): 311 – 320.

[22] Kurniawan T A, Lo W H, Chan G Y. Physico-chemical treatments for removal of recalcitrant contaminants from landfill leachate[J]. J Hazard Mater, 2006, 129(1 – 3): 80 – 100.

[23] Allegre C, Moulin P, Maisseu M, *et al.* Treatment and reuse of reactive dyeing effluents[J]. Journal of Membrane Science, 2006, 269(1 – 2): 15 – 34.

[24] Luo J Q, Ding L H, Su Y, *et al.* Concentration polarization in concentrated saline solution during desalination of iron dextran by nanofiltration[J]. Journal of Membrane Science, 2010, 363(1 – 2): 170 – 179.

[25] Van Der Bruggen B, Vandecasteele C. Removal of pollutants from surface water and groundwater by nanofiltration: overview of possible applications in the drinking water industry[J]. Environ Pollut, 2003, 122(3): 435 – 45.

[26] Li Y, Zhao Y J, Wang M. Effects of pH and salinity on the separation of magnesium and lithium from brine by nanofiltration[J]. Desalination and Water Treatment, 2017, 97: 141 – 150.

[27] Perezgonzalez A, Ibanez R, Gomez P, *et al.* Nanofiltration separation of polyvalent and monovalent anions in desalination brines[J]. Journal of Membrane Science, 2015, 473: 16 – 27.

[28] Wen X, Ma P, Chaoliang Z, *et al.* Preliminary study on recovering lithium chloride from lithium-containing waters by nanofiltration[J]. Separation and Purification Technology, 2006, 49(3): 230 – 236.

[29] Xiang W, Liang S K, Zhou Z Y, *et al.* Extraction of lithium from salt lake brine containing borate anion and high concentration of magnesium[J]. Hydrometallurgy, 2016, 166: 9 – 15.

[30] Lou Y, Chen Y, Wang S, *et al.* Application of membrane process to electroplating nickle effluent treatment[J]. 2002.

[31] Zhi W, Liu G, Fan Z, et al. Experimental study on treatment of electroplating wastewater by nanofiltration[J]. 305(1 – 2): 185 – 195.

[32] Junhe H J L C Y. Treatment of wastewater containing chromium ions with nanofiltration membrane[J]. CHEMICAL ENGINEERING(CHINA), 2013, 41(5): 64 – 68.

[33] Zhong Chang- Ming F X – H, Xu Zhen – Liang Treatment of Acidity Mining Wastewater by Nanofiltration Membrane[J]. Environmental Science and Technology, 2007, 30(7): 10 – 13.

[34] Wang J, Sun P, Fang F, *et al.* Treatment of acidic waste liquid containing metallic ions with membrane separation technology[J], 2010.

[35] Riitta K, Pertti K. Combination of membrane technology and limestone filtration to control drinking water quality[J]. Desalination, 2000, 131(1): 271 – 283.

[36] Somrani A, Hamzaoui A H, Pontie M. Study on lithium separation from salt lake brines by nanofiltration (NF) and low pressure reverse osmosis (LPRO)[J]. Desalination, 2013,

317(7): 184 - 192.
[37] Huang J, Chao L I, Yang J H. Treatment of wastewater containing chromium ions with nanofiltration membrane[J]. Chemical Engineering, 2013.
[38] Luo J, Wan Y. Effects of pH and salt on nanofiltration-a critical review[J]. Journal of Membrane Science, 2013, 438: 18 - 28.
[39] Elimelech M, Chen W H, Waypa J J. Measuring the Zeta (Electrokinetic) Potential of Reverse-Osmosis Membranes by a Streaming Potential Analyzer[J]. Desalination, 1994, 95(3): 269 - 286.
[40] Kedem O, Katchalsky A. Permeability of composite membranes. Part 2. —Parallel elements[J]. Transactions of the Faraday Society, 1963, 59(488): 1931.
[41] Straatsma J, Bargeman G, Van Der Horst H C, *et al.* Can nanofiltration be fully predicted by a model?[J]. Journal of Membrane Science, 2002, 198(2): 273 - 284.
[42] Van Der Bruggen B, Schaep J, Wilms D, *et al.* Influence of molecular size, polarity and charge on the retention of organic molecules by nanofiltration[J]. Journal of Membrane Science, 1999, 156(1): 29 - 41.
[43] Bowen W R, Mohammad A W. Diafiltration by nanofiltration: Prediction and optimization[J]. Aiche Journal, 1998, 44(8): 1799 - 1812.
[44] Szymczyk A, Fievet P. Investigating transport properties of nanofiltration membranes by means of a steric, electric and dielectric exclusion model[J]. Journal of Membrane Science, 2005, 252(1 - 2): 77 - 88.
[45] Szymczyk A, Fievet P. Ion transport through nanofiltration membranes: the steric, electric and dielectric exclusion model[J]. Desalination, 2006, 200(1 - 3): 122 - 124.
[46] Condom S, Larbot A, Younssi S A, *et al.* Use of ultra- and nanofiltration ceramic membranes for desalination[J]. Desalination, 2007, 168(1): 207 - 213.
[47] Bandini S, Drei J, Vezzani D. The role of pH and concentration on the ion rejection in polyamide nanofiltration membranes[J]. Journal of Membrane Science, 2005, 264(1 - 2): 65 - 74.
[48] Nightingale E R. Phenomenological Theory of Ion Solvation - Effective Radii of Hydrated Ions[J]. Journal of Physical Chemistry, 1959, 63(9): 1381 - 1387.
[49] Wang D X, Su M, Yu Z Y, *et al.* Separation performance of a nanofiltration membrane influenced by species and concentration of ions[J]. Desalination, 2005, 175(2): 219 - 225.
[50] Mazzoni C, Bruni L, Bandini S. Nanofiltration: Role of the Electrolyte and pH on Desal DK Performances +[J]. Industrial & Engineering Chemistry Research, 2007, 46(8): 2254 - 2262.
[51] Coday B D, Luxbacher T, Childress A E, *et al.* Indirect determination of zeta potential at high ionic strength: Specific application to semipermeable polymeric membranes[J]. Journal of Membrane Science, 2015, 478: 58 - 64.
[52] Bi Q, Zhang Z, Zhao C, *et al.* Study on the recovery of lithium from high Mg(2 +)/Li(+) ratio brine by nanofiltration[J]. Water Sci Technol, 2014, 70(10): 1690 - 4.

纳滤法用于铝锂分离的初步研究

高 琳[1,2,3],王怀有[1,2*],赵有璟[1,2],王 敏[1,2*]
(1. 中国科学院青海盐湖研究所,中国科学院盐湖资源综合高效利用重点实验室,青海 西宁 810008;
2. 青海省盐湖资源化学重点实验室,青海 西宁 810008;3. 中国科学院大学,北京 101408)

摘 要:本文探讨了纳滤分离 Al^{3+} 和 Li^{+} 的可行性,研究了含盐量和铝锂比对分离效率的影响,提出了从锂云母浸出液中分离回收锂的新方法。实验结果表明,纳滤膜对 Al^{3+} 和 Li^{+} 的截留率随含盐量的升高而降低,其中 Li^{+} 始终呈现负浓度梯度扩散的趋势,而 Al^{3+} 的截留率始终稳定在99%以上。当含盐量为45 g/L时,铝锂分离因子最高可达248.33,膜面相应Zeta电位的绝对值达到最大。随着溶液中铝锂比的变化,Al^{3+} 和 Li^{+} 的截留率分别在不同铝锂比的条件下出现拐点,溶液的pH呈现先下降后上升最后下降的复杂趋势。本实验研究发现,DK膜能够在酸性环境下实现高效的铝锂分离和锂的浓缩,从而为锂云母浸出液中锂的提取提供新的思路。

关键词:纳滤;铝分离;提锂;Zeta电位;锂云母浸出液